American Journal of Pathology, Vol. 164, No. 4, April 2004

Suppression of Tumor Growth and Angiogenesis *in Vivo* by a Truncated Form of 24-kd Fibroblast Growth Factor (FGF)-2

Eugene G. Levin, Lyudmila Sikora, Lan Ding, Savita P. Rao, and P. Sriramarao

From the Division of Vascular Biology, La Jolla Institute for Molecular Medicine, San Diego, California

Efforts to treat tumors have routinely depended on disruption of cell proliferation by a variety of methods, many involving stimulation of apoptosis. We have previously shown that a truncated form of 24-kd basic fibroblast growth factor consisting of the amino terminal 86 amino acids inhibits migration of tumor and endothelial cells *in vitro*. In the present study, this peptide was tested for its ability to suppress angiogenesis and tumor growth using the murine dorsal skin-fold chamber model *in vivo*. Treatment of MCF-7 breast carcinoma tumor spheroids with this peptide resulted in cessation of the angiogenic response and a significant reduction in tumor size. Blood vessels that did form were poorly developed. In addition to inhibiting angiogenesis, the peptide also inhibited migration of Lewis lung carcinoma cells away from the tumor core before onset of angiogenesis indicating that the peptide-mediated inhibition of migration affects both angiogenesis and tumor growth independently. Despite inhibition of tumor cell migration, the peptide had no effect on neutrophil or eosinophil chemotaxis. This study demonstrates that the truncated form of 24-kd basic fibroblast growth factor is effective in suppressing tumor development *in vivo* through inhibition of angiogenesis as well as inhibition of tumor cell migration without compromising other homeostatic events. *(Am J Pathol 2004, 164:1183–1190)*

Basic fibroblast growth factor (FGF)-2 is a mitogen that is produced and secreted by endothelial cells and which promotes cell proliferation, chemotaxis, protease production, and integrin expression.[1–4] FGF-2 has been implicated in cell proliferation and migration during development, apoptosis, wound healing, tumor growth, and angiogenesis.[1,5–10] A single copy gene for FGF-2 encodes for multiple forms of the protein of molecular weights 24, 22.5, 22, and 18 kd, with the three higher molecular weight isoforms being produced by initiation of translation at three CUG codons located upstream from the classical AUG initiation site.[11,12] 24-kd FGF-2 consists of the 18-kd isoform plus an additional 55 amino acids at the amino terminal end (ATE).

We have previously demonstrated that endothelial cells can be stimulated to secrete the high molecular weight forms of FGF-2 in a regulated manner to levels capable of affecting cell behavior.[13] The effects were twofold: stimulation of cell proliferation and inhibition of migration. The increase in proliferation was comparable to that promoted by 18-kd FGF-2, indicating that the stimulation of cell proliferation was independent of the additional amino terminal peptide. On the other hand, 24-kd FGF-2 inhibited migration of endothelial cells by 50% and mammary carcinoma MCF-7 cells by greater than 70%, even in the presence of unrelated mitogens such as vascular endothelial growth factor (VEGF) and insulin-like growth factor (IGF)-1 that promote cell migration. Overall, the 24-kd FGF-2 affects cell behavior differently than 18-kd FGF-2 and the ATE is responsible for this difference. Further studies from our laboratory using a series of truncated forms of 24-kd FGF-2 have demonstrated that the ability to induce cell proliferation is lost with the removal of 40 amino acids from the carboxy terminal end, while full ability to inhibit migration is retained. The smallest peptide generated which displayed maximal inhibition contained the ATE in addition to the first 31 amino acids of the 18-kd FGF-2 domain (ATE + 31).[14]

Migration is a fundamental cell behavior that is required for a number of physiological and pathological events such as angiogenesis,[15] tumor development and metastasis,[16,17] development,[18] and leukocytic transmigration.[19,20] Angiogenesis itself is involved in a variety of disease states, for example, tumor-dependent vascular formation and retinopathy.[21,22] In the present study we used the murine dorsal skin-fold window chamber model[23,24] to determine whether inhibition of migration by ATE + 31 could reduce angiogenesis and tumor growth *in*

Supported in part by funding from Breast Cancer Research Program grant 4JB-0164 and NIH 1RO1AI35796 (to P.S.) and NIH 1RO1CA81209 (to E.G.L.).

Accepted for publication December 9, 2003.

Address reprint requests to P. Sriramarao, Ph.D., and/or Eugene G. Levin, Ph.D., Division of Vascular Biology, La Jolla Institute for Molecular Medicine, 4570 Executive Drive, San Diego, CA 92121. E-mail: glevin@ljimm.org.

vivo. This model provides microscopic access to the vasculature of the skeletal skin muscle and subcutaneous connective tissue. It allows the implantation of multicellular aggregates made up of any of a variety of tumor cells within the chamber and enables monitoring of the tumor and its microcirculation over time in response to peptide treatment. Thus, we have the ability to measure changes in tumor characteristics at any point during the experiment and to generate a true picture of how a single tumor aggregate responds to the protein peptide over a prolonged period. Another advantage of this technique is that it overcomes the problems associated with endpoint analysis with multiple animals and the uncertainty of animal-to-animal variation. The results presented in this paper demonstrate that ATE + 31 is a potent inhibitor of both angiogenesis and tumor growth while, more importantly, failing to affect cellular events such as chemotaxis of inflammatory cells like neutrophils and eosinophils.

Materials and Methods

Construction and Expression of 24-kd FGF-2 and Its Mutated Forms

To generate pure recombinant 24-kd FGF-2, full-length 24-kd FGF-2 cDNA was inserted in frame into a pPIC9K yeast expression vector (Invitrogen, San Diego, CA) between the SnaBI and AvrII restriction sites of the pPIC9K vector directly downstream of the DNA encoding the X-factor secretion signal region. The His4 mutant of *P. pastoris* GS 115, the methanol-utilization-positive phenotype (Mut+), was transformed by electroporation with the pPIC9K construct vector linearized with *Sac*I. The His+ yeast transformants were grown on minimal dextrose medium (MD) plates and those carrying the kanT gene further selected for multiple integrated copies by replating on plates containing 4.0 mg/ml G418 antibiotic. The multicopy transformant was grown in 50 ml BMGY medium with glycerol as the sole carbon source until the cultures reached an $OD_{600} = 2$ to 6 (approximately 16 to 18 hours). The cells were collected by centrifugation at 1500 to 3000 $\times$ *g* for 5 minutes at room temperature and the cell pellet resuspended in BMGY medium to induce expression. The cells were grown for 4 days and 100% methanol was added every 24 hours to a final concentration of 2% to maintain protein expression. The medium was cleared of the yeast by filtration and mixed with 5 ml heparin-Sepharose for 2 hours at 4°C. The gel was washed with 50 ml buffer A [20 mmol/L Tris-HC1, 5 mmol/L EDTA, 2 mmol/L EGTA (pH 7.4)] and then with buffer A containing 0.5 mol/L NaCl. The recombinant 24-kd FGF was eluted with buffer A containing 3 mol/L NaCl. The eluate was dialyzed against 4 liters of 20 mmol/L Tris, 145 mmol/L NaCl (pH 7.4).

ATE + 31 was prepared by inserting *Sfi*I restriction sites at the 5′end of the 24-kd FGF-2 cDNA and the 3′ end of the sequence generating the required truncation of 24-kd FGF-2. The cDNA fragment was amplified by PCR and inserted into a modified pET15b vector carrying an N-terminal pelB signal sequence for periplasmic localization of the recombinant protein plus a C-terminal His-Tag sequence. The 5′ primer was 5′-ATATATGGCCCAGC CGGCCATGGCACTGGGGGACCGCGGGCGCGG-3′ (*Sfi*I restriction site underlined) and the 3′-primer was 3′-ATATATGGCCCCCGAGGCCCCGCCTTGGGGTCCTTGAAGTGG-5′. The amplified fragments were cut with *Sfi*I and ligated to the vector. The plasmids were used to transform BL-21-CodonPlus (DE-3)-RP competent cells. The cells were cultured in LB medium containing 0.4 mmol/L isopropyl-β-D-thiogalacto pyranoside (IPTG) for 4 hours at 30°C. When the OD_{600} value of the culture reached 0.6 to 0.8, the cells were harvested and suspended in 50 mmol/L phosphate-buffered saline (PBS), 10% glycerol, 300 mmol/L NaCl, 5 mmol/L 2-mercaptoethanol; pH 8.0 (buffer B). The cells were lysed by freeze-thaw five times and the particulate matter removed by centrifugation and filtration through a 0.45-μm syringe filter. The filtrate was added to 5 ml of nickel-NTA agarose and the mixture shaken for 2 hours at 4°C. The resin was packed into a column and washed with buffer B containing 10 mmol/L imidazole, followed by the same buffer containing 50 mmol/L imidazole and the protein was finally eluted with buffer containing 400 mmol/L imidazole. The protein was dialyzed against 50 mmol/L sodium phosphate (pH 7.6) and analyzed by 10% SDS-PAGE followed by silver staining and Western blot analysis using antibodies generated against a 12-amino acid peptide found within the ATE domain of 24-kd FGF-2.[13]

Cell Culture and Migration Assay

MCF-7 breast carcinoma cells or Lewis lung carcinoma (LLC) cells were maintained in Dulbecco's minimal essential media (DMEM) supplemented with 1 mmol/L sodium pyruvate, 10% fetal calf serum, and 1X penicillin/streptomycin at 37°C under 5% CO_2 in humidified incubators. The cells were subcultured to densities of one-third to one-sixth that of confluent cultures.

For migration assays, MCF-7 cells were harvested with trypsin, counted, centrifuged, and resuspended at a cell density of 1×10^5 cells in 0.5 ml DMEM containing 0.5% bovine serum albumin (BSA). Cells were added to the upper well of a 6.5-mm Transwell microporous filter chamber (Fisher Scientific, Tustin, CA) containing an 8.0-μm pore size polycarbonate membrane, which separates the upper well from the lower well of the Transwell chamber. The filters were not coated with protein before use. The upper wells were placed into the lower wells containing 0.75 ml of DMEM with 0.5% BSA to which 10 ng/ml of IGF-1 (Sigma Chemical Co., St. Louis, MO) or VEGF (Sigma) was added as a chemoattractant. 24-kd FGF-2 or truncated forms of the protein was added to both wells of each chamber at the appropriate concentration. After 4 to 6 hours of incubation at 37°C in 5% CO_2, non-migratory cells on the upper membrane surface were removed with a cotton swab and the cells that traversed and spread on the lower surface of the filter were fixed and stained with Diff-Quik (Dade-Behring, Deerfield, IL). The filter was mounted on a glass slide, and four phase-contrast photomicrographs/membrane were taken at a

magnification of ×100. The number of cells per field was counted from contact sheets and the results compared with control chambers, which had no 24-kd FGF-2 added.

Chemotaxis of eosinophils and neutrophils was performed using the same system except that the upper well of the Transwell chamber contained a polyethylene terephthalate filter of 3.0-μm pore size, which separated it from the lower chamber. The membrane was coated with Matrigel. For each determination, neutrophils and eosinophils labeled with (5(and-6)-(((4-chloro-methyl-)benzoyl)amino)tetramethylrhodamine (CMTMR; Molecular Probes, Eugene, OR) were placed in the upper wells (10^5 labeled cells/well) of the chamber in the presence or absence of 1×10^{-7} M ATE + 31 or 10 μg/ml IB4. IB4, an antibody against $\beta 2$ integrin, was used as a positive control to demonstrate inhibition of migration. The lower well contained 1 mg/ml human serum albumin in DMEM with 1×10^{-7} M C5a. The chambers were incubated at 37°C for 2 hours. EDTA was added to a final concentration of 10 mmol/L to the bottom well, and the plates were allowed to stand for 10 minutes at room temperature before the inserts were removed from the wells. The cells, which had passed through the membrane and which were contained within a 1.1-mm^2 central area on the bottom well, were counted using an inverted fluorescence microscope (Leitz Fluovert FS, Wetzlar, Germany).

To measure growth rates, MCF-7 cells (6×10^3) were plated in growth medium for 48 hours after which the medium was changed to assay medium containing phenol red-free modified Eagle's medium (MEM) supplemented with 1 mmol/L sodium pyruvate and 0.3% lactalbumin hydrolysate with or without growth factors and the cultures were incubated for an additional 24 hours. Two hours before the termination of the experiment, ^{3}H-thymidine was added. The cultures were washed two times with PBS followed by ice-cold methanol and 5% trichloroacetic acid (two times for 10 minutes each), and the DNA was finally extracted with 0.3 N NaOH. The number of counts per minute (cpm) incorporated was determined by liquid scintillation.

Preparation of Tumor Spheroids

Multicellular aggregates or tumor spheroids were prepared by suspending cells at a concentration of 5×10^6 cells/ml in the appropriate growth medium in a 50-ml flask and the suspension rocked on a gyratory shaker in a humidified incubator at 37°C in an atmosphere of 5% CO_2 and 95% room air. Solid tumor spheroids are formed after 24 to 48 hours of shaking. Tumor spheroids with similar diameters (600 to 1000 μm) for implantation in the dorsal skin-fold chamber were selected by visualizing the spheroids under a microscope and individually picking the spheroids with a sterile pipette. This procedure insures single spheroids of similar size for implantation in the chamber. To facilitate visualization of the implanted tumors, spheroids were pre-labeled with CMTMR before transplantation into the skin-fold chamber.[25]

Dorsal Skin-Fold Chamber Model

To prepare the skin-fold chamber in mice, one layer of the dorsal skin was removed surgically and a pair of titanium frames were implanted into the dorsal skin-fold parallel to the dorsum creating a sandwich of the stretched layer of skin. The underlying thin layer of skin (M. cutaneous max.), subcutaneous tissue, and epidermis was covered with a coverslip enclosed in one of the frames and the animals allowed to recover from anesthesia.[24–26] After an additional convalescence period of 2 to 3 days, the coverslip was removed and tumor spheroids were placed over the upper tissue layer of the chamber. The chamber was enclosed with the coverslip and the tumor spheroids were monitored over a 2-week period.

Evaluation of Tumor Development

The progress of tumor development and vascularization were followed by intravital microscopy. Unanesthetized mice containing the tumor spheroids were placed individually in a crouched position in a plexiglass tube and then placed on a microscope stage (Leitz Biomed) for observation of the tumor spheroids within the chamber. On the day of spheroid implantation, an overview video print was taken and the position of the implanted spheroids marked to facilitate future localization and for monitoring growth of the tumor. The CMTMR-labeled tumor spheroids and angiogenic blood vessels were observed by transillumination or stroboscopic epi-illumination using a video-triggered Xenon arc and a Leitz Ploemopak epi-illuminator. Tumor size was determined by measuring the diameter of the tumors at each time point and tumor volume was calculated according to the formula V = 2/3AH where A is the tumor area and H the thickness of the tumor. At the end of each experiment, the tissue containing the tumors was excised, fixed in 10% formalin, and prepared for sectioning by freezing in OCT. Ten-μm sections of the surrounding skin were also prepared and stained with hematoxylin-eosin (HE).

Results

ATE + 31 Inhibits the Development of Tumors of MCF-7 Breast Carcinoma Cells

ATE + 31 was generated by deletion mutagenesis through the placement of a stop codon within the 24-kd FGF-2 cDNA after amino acid 86 (Figure 1 A). Figure 1B shows the effect of ATE + 31 on MCF-7 cell proliferation and migration compared to the full-length 24-kd FGF-2. At the optimum dose of 3.3×10^{-10} M, migration rates are reduced by 80% which is equal to the maximum inhibition by the full length 24-kd FGF-2.[14] However, in contrast to the increase in proliferation induced by 24-kd FGF-2, ATE + 31 has no effect on the rate of cell growth when compared to untreated MCF-7 cells (Figure 1B)[14]. To determine whether ATE + 31 is effective in limiting tumor angiogenesis *in vivo*, MCF-7 cell spheriods (microtumors) were implanted into skin-fold chambers in mice

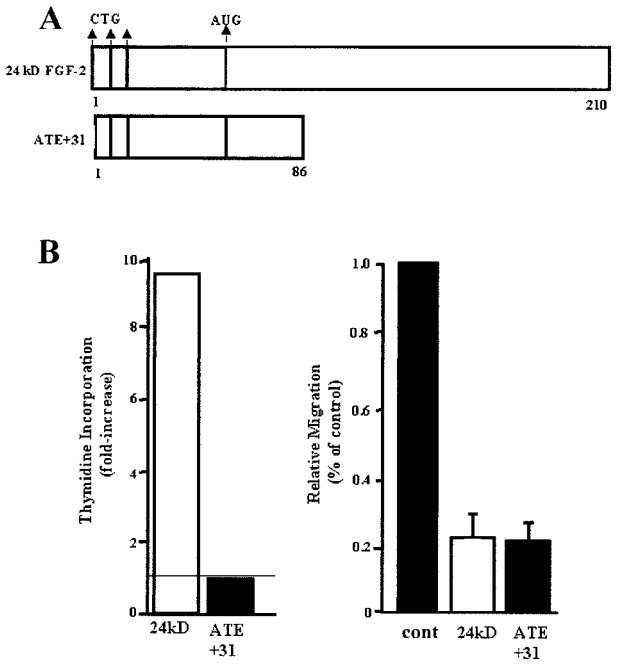

Figure 1. A: Schematic diagram of 24-kd FGF-2 and its truncated form ATE + 31. The three CTG translation initiation sites are shown at the ATE. The AUG translation initiation site represents the ATE of 18-kd FGF-2. **B:** The effects of 24-kd FGF-2 and ATE + 31 on MCF-7 cell migration in a Boyden Chamber assay (**right panel**) and cell proliferation (**left panel**) were tested. ATE + 31 at 3.3×10^{-10} M and 24-kd FGF-2 at 6.6×10^{-11} M were used and the cell migration rates in response to 10 ng/ml IGF-1 were measured. Uncoated filters were used in this study. Results are presented as a percentage of the migration rate of MCF-7 cells in the presence of 10 ng/ml IGF-1 alone and represent the average ± SD of at least three separate experiments. Dose response experiments are described in Reference 14. The effect of ATE + 31 and 24-kd FGF-2 on proliferation of MCF-7 cells was determined at the same concentrations by measuring the rate of thymidine incorporation. 24-kd FGF-2 stimulated thymidine incorporation 8- to 10-fold while ATE + 31 had no effect. Results are presented relative to the rate of thymidine incorporation in the absence of any growth factor (indicated by the **horizontal line**) and represent the average of two experiments.

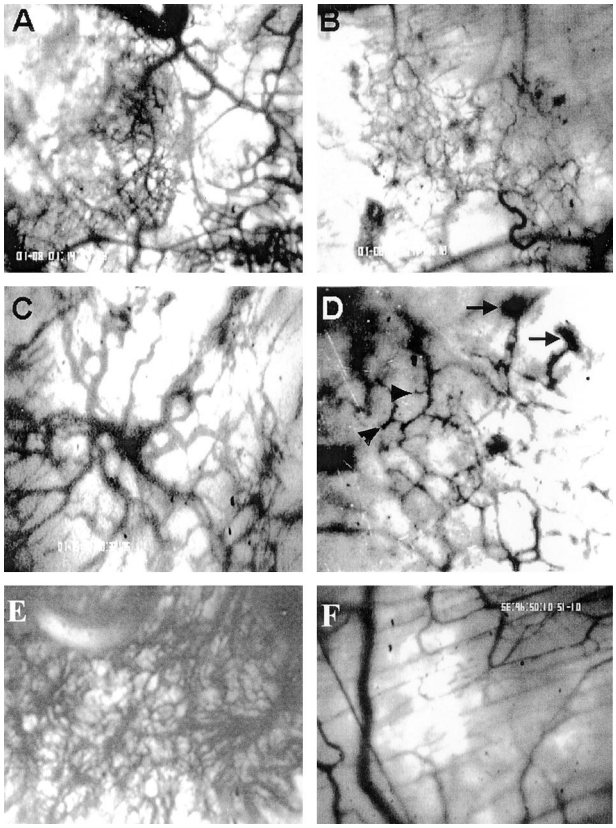

Figure 2. Effect of ATE + 31 on MCF-7 tumor angiogenesis. Spheroids containing MCF-7 cells were placed within dorsal skin-fold chambers and locally treated (superfused) with 20 ng of ATE + 31 in 20 μl saline or an identical volume of saline alone at 24 hours and every 2 days after. Vascular development was followed by intravital microscopy. **A–D:** Angiogenesis after 5 days. **A:** Control, showing robust vascular infiltration. **B:** ATE + 31-treated, demonstrating little neovascularization. Magnification, ×40. **C** and **D:** The integrity of the newly formed blood vessels appears to be aberrant in ATE + 31-treated tumors. Vessels within treated tumors (**D**) appear fractured and in certain cases end precipitously (**arrowheads**) or in a mass of poorly formed vessels (**arrows**) compared to vessels within untreated tumors (**C**). Magnification, ×100. **E** and **F:** Angiogenesis after 15 days. The untreated tumor (**E**) has a much richer vascular network than the ATE + 31-treated tumor (**F**). Magnification, ×100.

and treated by superfusion with 20 ng ATE + 31 (or saline control) at 24 hours and every 2 days after. The infiltration of new blood vessels into the spheroid was observed by video microscopy. By day 5 the density of the neovasculature within the area of the spheroid exposed to ATE + 31 (Figure 2 B) was significantly less than that of the saline-treated spheroids (Figure 2A). The integrity of the growing vessels was also affected by the presence of the peptide (Figure 2, C and D). The vasculature in ATE-31-treated tumors contained fragmented vessels (arrowheads), an effect we attribute to the formation of poorly differentiated blood vessels (arrows, Figure 2D). Differences in vascular density were further magnified by day 15. The vascular plexus in the untreated animals was extremely dense filling up most of the space within the spheroid (Figure 2E), whereas the treated animals, while showing a small increase in the number of blood vessels compared to that observed on day 5, had few blood vessels with large diameters such as those found in control animals (Figure 2F).

The extent of tumor growth suppression induced by ATE + 31 was evaluated by histological examination of the area within the skin-fold chamber on day 15 (Figure 3). A dramatic decrease in tumor size was observed in the treated animals with the average size of the treated tumors 7.8% that of the control spheroids (1.3 mm^2 *vs.* 16.8 mm^2, $n = 3$) after 15 days (Figure 3, A *versus* B). Blood vessels infiltrating the interior of the untreated tumor are visible in contrast to the treated tumor, where almost none are discernable (Figure 3, C and D, respectively). Variation in final tumor size does occur and some animals were found to have no tumor at all by day 15 indicating that tumor maintenance is also compromised by the peptide, either by directly affecting tumor cell migration or through the inhibition of blood vessel formation.

The efficacy of the peptide on LLC cells was also tested. The purpose of these experiments was to determine whether ATE + 31 would be effective against a faster growing and more aggressive tumor cell and whether the effect of suppressing spheroid growth could be independent of angiogenesis. CMTMR-labeled LLC cell spheroids were implanted into the skin-fold chamber and spheroid size was monitored by intravital microscopy

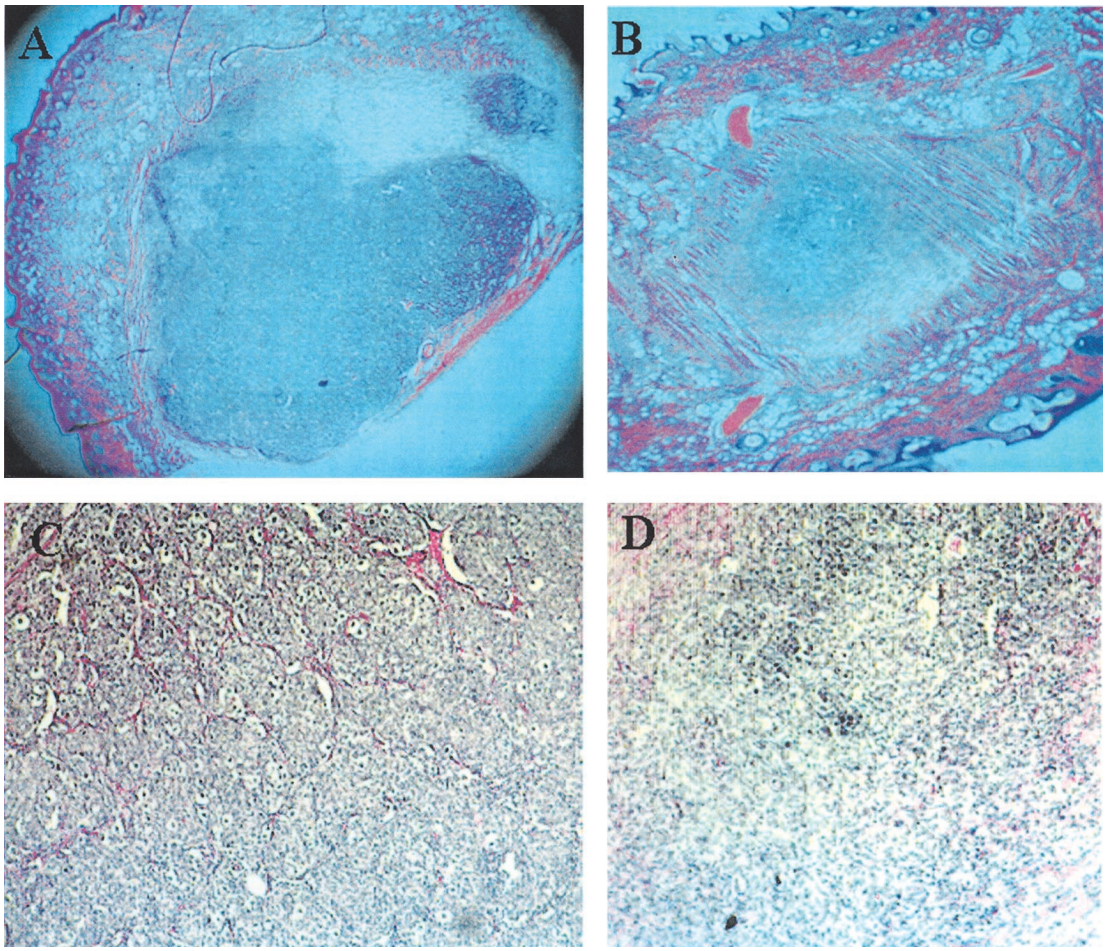

Figure 3. Histological evaluation of MCF-7 tumors after ATE + 31 treatment. Tissue containing the tumor spheroid, with and without treatment with ATE + 31, was excised after 15 days, fixed, sectioned, and stained with H&E. A comparison of control (**A**) and ATE + 31-treated (**B**) tumors shows a dramatic difference in tumor size. Magnification, ×25. A section from untreated tumors under higher magnification (**C**) shows an abundant vascular supply (stained red) infiltrating the tumor from the surrounding tissue while few vessels can be seen in the section from the ATE + 31-treated tumors (**D**). Magnification, ×100.

using stroboscopic epi-illumination (Figure 4). Treatment with ATE + 31 at 20 ng as described earlier did not result in significant suppression of the tumor growth. However, when the concentration of ATE + 31 was increased to 100 ng, a dramatic effect on growth was observed. Over the first 7 days, untreated tumor spheroids grew in size ninefold (0.26 ± 0.05 mm^3 to 2.5 ± 0.6 mm^3), while the treated spheroids showed only a threefold increase (to 0.9 ± 0.3 mm^3). After day 7, there was a further increase in the rate of tumor expansion in untreated animals with a final tumor volume 28 times larger than that of the original spheroid (8.5 ± 3.9 mm^3) (Figure 4A). In contrast, significant suppression (81%) of tumor growth was observed in the ATE + 31-treated animals (1.5 ± 0.2 mm^3) compared to the untreated tumor. Thus, ATE + 31 was most effective during the period of rapid tumor growth. This effect was also reflected in the vascularization of the tumor (Figure 4, B to E). At 6 days after implantation, a dense network of angiogenic blood vessels was seen in saline-treated control animals (Figure 4, B and D), while the area containing newly formed blood vessels in ATE + 31-treated animals was small, diffuse, and poorly developed (Figure 4, C and E).

The rapid growth rate of LLC cells enabled us to determine whether ATE + 31 can suppress the growth of tumors independently of its inhibition of angiogenesis. This allows us to measure increase in spheroid size before the infiltration of angiogenic blood vessels into the tumor itself (which occurs 2 to 3 days after implantation).[25] Spheroids of fluorescently labeled cells appear as intensely fluorescent bodies with distinct margins immediately after placing them in the chamber (Figure 5A). After 48 hours, the spheroid in control animals spreads into a much larger and very diffuse structure without an inner core (Figure 5B) and was found to increase in size by threefold (19.8 ± 2.4 *vs.* 6.9 ± 1.6 mm^2, Figure 5D). However, treatment with ATE + 31 mitigates this expansion and the spheroid body remains intact (Figure 5C) with only a small halo of cells around it after 48 hours (6.1 ± 0.5 *vs.* 6.9 ± 1.6 mm^2, Figure 5D). Thus, suppression of tumor growth can occur even in the absence of a vascular system indicating that ATE + 31 is more than an anti-angiogenic molecule and functions via inhibition of tumor cell migration.

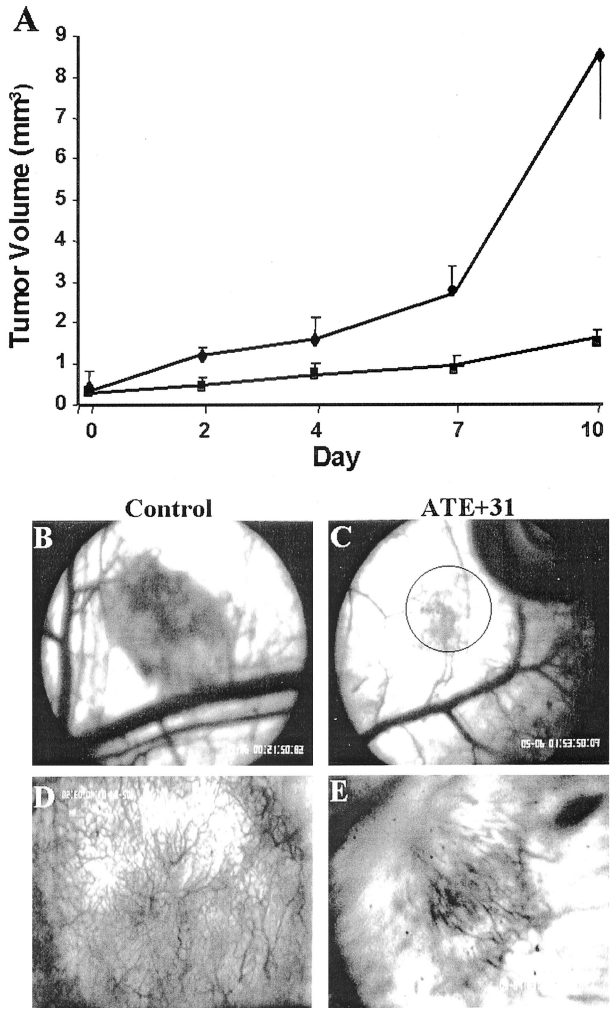

Figure 4. ATE + 31 inhibits the growth and vascularization of LLC tumors. **A:** Spheroids consisting of LLC cells labeled with CMTMR were implanted in the skin-fold chamber and treated with vehicle as a control (♦) or 100 ng of ATE + 31 (■) every 48 hours for 10 days. At the days indicated the tumors were video recorded and tumor volume measured by offline analysis. Volume of treated tumors on day 10 was less than 20% of that of untreated tumors. Results represent the average ± SD of at least five tumors each from different mice. **B–E:** Angiogenic response of LLC tumors. Six days after implantation, vascular development in control (**B** and **D**) and ATE + 31-treated (**C** and **E**) tumors was analyzed by video microscopy at lower (**B** and **C**, ×40) and higher (**D** and **E**, ×100) magnification. The area of vasculature is indicative of the difference in size between the two tumors. The **circle** in **C** shows the area analyzed in **E**.

ATE + 31 Does Not Affect Leukocyte Transmigration

While the inhibition of migration of endothelial and tumor cells is an advantage for suppressing tumor growth, its effect on other physiological processes such as leukocyte trafficking would be detrimental to the immune system. To determine whether leukocyte motility is affected by ATE + 31, *in vitro* chemotaxis experiments were performed with peripheral blood human eosinophils and polymorphonuclear neutrophils (Figure 6). In the presence of C5a,[27] the number of migrating neutrophils increased from 6.5 ± 1.5% to 11.6 ± 2.0% and this did not change when ATE + 31 was added (12.0 ± 3.0%) (Figure 6A). IB4, a function blocking monoclonal antibody

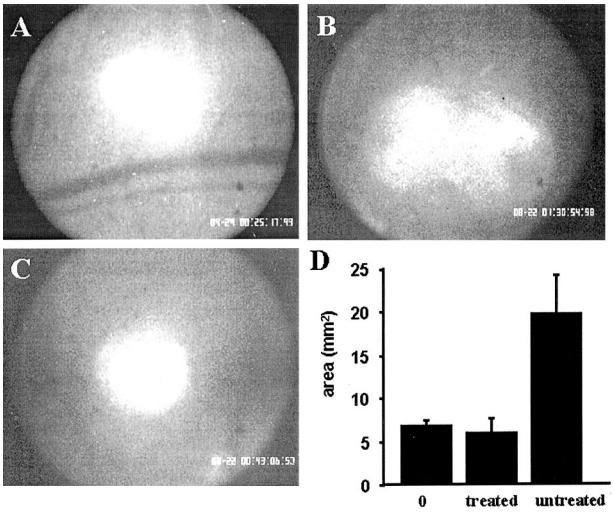

Figure 5. Evaluation of CMTMR-labeled LLC tumors 48 hours after implantation. Before the invading blood vessels have infiltrated the tumor, the distribution of the fluorescently labeled cells was recorded and area quantified. **A:** Tumor immediately after implantation (day 0). **B:** Control tumor 48 hours after implantation. **C:** ATE + 31-treated tumor 48 hours after implantation. **D:** Comparison of the average area ± SD of treated and control tumors; n = 2 to 3 tumors/animal in five different mice. Compared to the implanted tumor on day 0, little expansion of the treated tumor was observed after 48 hours.

against CD18, reduced neutrophil migration to 3.8 ± 0.9%. Similar results were observed with eosinophils, where the number of migrating cells increased from 18.8 ± 1.0% to 28.4 ± 1.7% in the presence of C5a. While treatment with IB4 resulted in complete inhibition of chemotaxis (17.5 ± 1.5%), the presence of ATE + 31 failed to alter the C5a-induced migration of eosinophils (28.8 ± 3.0%) (Figure 6B).

Discussion

Much of the development of anti-tumor therapy has focused on the attenuation of the angiogenic response to tumor growth or the suppression of tumor cell proliferation.[28] Both of these approaches have largely depended

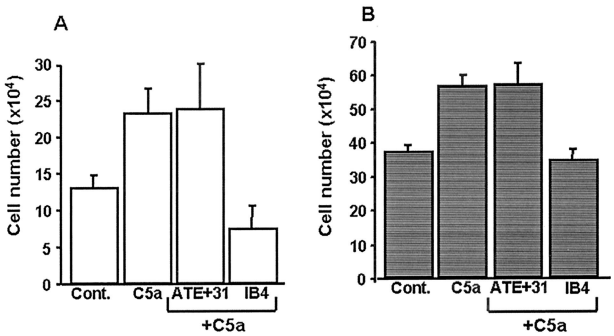

Figure 6. Chemotaxis of human neutrophils and eosinophils is not affected by ATE + 31. Chemotaxis assays were performed with 1×10^5 neutrophils (**A**) or eosinophils (**B**) using complement factor C5a as the chemoattractant. The ability of ATE + 31 to inhibit chemotaxis was tested at a concentration of 1×10^{-7} M. IB4, an antibody that binds to the $\beta 2$ integrin and inhibits the migration of neutrophils and eosinophils, was used as the positive control. ATE + 31 had no effect on either neutrophil or eosinophil chemotaxis. Results represent the average ± SD of four (eosinophils) or eight (neutrophils) experiments.

on causing cell death, eg, through the use of cytotoxic compounds specifically targeted to tumor or endothelial cells.[29] However, suppression of tumor development and angiogenesis through the regulation of tumor and endothelial cell motility has rarely been considered as an additional or alternative approach to therapy. Cell migration is a pivotal component of the formation and growth of any tissue from the very beginning of fetal development to wound repair, inflammatory response, angiogenesis, and tumor growth and metastasis. With that in mind, we have tested the efficacy of a truncated form of 24-kd FGF-2 consisting of 86 amino acids from the ATE on tumor growth and angiogenesis in an animal model. This peptide has the ability to inhibit cell migration of both endothelial cells and tumor cells *in vitro* even in the presence of mitogens that promote enhanced migration.[14] Therefore, we proposed that this peptide would inhibit tumor formation by inhibiting movement of endothelial cells necessary for formation of angiogenic blood vessels as well as the motility of tumor cells that must occur for expansion of the tumor and continued tumor cell proliferation.

In this study we analyzed the effect of ATE + 31 on LLC and MCF-7 tumor growth and angiogenesis using the dorsal skin-fold chamber model. This model allows us to monitor vascular development as well as the growth rate of a single well-defined microtumor over a period of time. We demonstrated that ATE + 31 is effective not only at suppressing tumor-induced angiogenesis, but tumor growth itself in the absence of a vascular network. When LLC cells were used, the final tumor volume after 10 days was less than 20% of saline-treated tumors (80% inhibition) while with MCF-7 cells the tumor was only 8% of saline-treated control tumors (>90% inhibition). These results support our hypothesis that inhibition of migration can lead to suppression of tumor growth involving very different types of cells *in vivo*. Equally important is the observation that suppression of tumor growth is not merely a consequence of inhibition of angiogenesis but is also due to an effect on the tumor cells themselves. This was indicated by the suppression of microtumor expansion even before the infiltration of blood vessels. Since we have shown that ATE + 31 does not affect proliferation,[14] we interpret the differences in the sizes of the tumors and the diminished vascularization as a consequence of inhibition of migration. Suppressing tumor development through the inhibition of migration must address the possibility that other physiological processes that depend on cell motility would be compromised. One of the most crucial is the ability of blood cells to transmigrate into the vessel wall in response to inflammatory events. The results shown in Figure 6 demonstrate that ATE + 31 has no effect on the transmigration of either neutrophils or eosinophils in an *in vitro* chemotaxis assay. These experiments were performed under similar conditions as those using endothelial cells and MCF-7 cells so that the only variable was the cells themselves. Thus, despite the apparent widespread effect of ATE + 31 on endothelial cells and tumor cells, the mechanism by which it inhibits these cells is not applicable to leukocytes, a property that serves as an advantage for therapeutic use.

The mechanism through which ATE + 31 inhibits migration has not been elucidated although competition binding studies with the 24-kd FGF-2 and 18-kd FGF-2 indicate that it occurs independently of the FGF receptor[14] and that the truncated protein does not contain a site that interferes with the binding of the full-length 24-kd FGF-2 to its receptor. ATE + 31 does bind MCF-7 cells in a specific and saturable manner suggesting that it has its own receptor/binding site distinct from the FGF receptor (unpublished observation). Since the inhibition of migration by ATE + 31 occurs in the presence of three unrelated growth factors, it is very likely that this protein affects the cells through a common point downstream of ligand-receptor interaction although neither extracellular signal-related kinase (ERK) nor AKT phosphorylation are affected by treatment with this protein.[14] This still leaves a multitude of events that affect the mechanics of movement, eg, by altering cytoskeletal dynamics or adhesion. In fact, preliminary studies of the adhesive properties of treated *versus* untreated MCF-7 cells show an increase in adhesion to fibronectin, collagen, and laminin. For cells to migrate, they must adhere to and release from the substratum in a coordinated and polarized fashion. This process involves formation of filopodia and lamellipodia at the leading edge, formation of new adhesions in this region, and detachment of adhesions at the trailing edge of the cell.[30,31] The inability to release these contacts at the required rate would compromise the motility of the cells leading to suppression of vascular formation or tumor growth. These studies demonstrate the pronounced effect that inhibition of migration can have on the growth of tumors and blood vessels.

In summary, this study demonstrates that ATE + 31 effectively inhibits both growth and neovascularization of various types of tumors potentially through the inhibition of migration of tumor cells. In contrast, ATE + 31 fails to affect the transmigration of neutrophils and eosinophils, indicating that this molecule specifically acts against tumor cells but not inflammatory leukocytes. These results suggest that ATE + 31 has the potential to function as an anti-tumor agent with multiple targets.

References

1. Slavin J: Fibroblast growth factors: at the heart of angiogenesis. Cell Biol Int Rep 1995, 19:431–444
2. Moscatelli D, Presta M, Rifkin DB: Purification of a factor from human placenta that stimulates capillary endothelial cell protease production, DNA synthesis, and migration. Proc Natl Acad Sci USA 1986, 83:2091–2095
3. Presta M, Moscatelli D, Joseph-Silverstein J, Rifkin DB: Purification from a human hepatoma cell line of a basic fibroblast growth factor-like molecule that stimulates capillary endothelial cell plasminogen activator production, DNA synthesis, and migration. Mol Cell Biol 1986, 6:4060–4066
4. Pepper MS, Meda P: Basic fibroblast growth factor increases junctional communication and connexin 43 expression in microvascular endothelial cells. J Cell Physiol 1992, 153:196–205
5. Becker D, Meier CB, Herlyn M: Proliferation of human malignant melanomas is inhibited by antisense oligodeoxynucleotides targeted against basic fibroblast growth factor. EMBO J 1989, 8:3685–3691
6. Presta M: Sex hormones modulate the synthesis of basic fibroblast growth factor in human endometrial adenocarcinoma cells: implica-

tions for the neovascularization of normal and neoplastic endometrium. J Cell Physiol 1988, 137:593–597
7. Yang W, De Bono DP: A new role for vascular endothelial growth factor and fibroblast growth factors: increasing endothelial resistance to oxidative stress. FEBS Lett 1997, 403:139–142
8. Mignatti P, Tsuboi R, Robbins E, Rifkin DB: In vitro angiogenesis on the human amniotic membrane: requirement for basic fibroblast growth factor-induced proteinases. J Cell Biol 1989, 108:671–682
9. Fox JC, Shanley JR: Antisense inhibition of basic fibroblast growth factor induces apoptosis in vascular smooth muscle cells. J Biol Chem 1996, 271:12578–12584
10. Gardner AM, Johnson GL: Fibroblast growth factor-2 suppression of tumor necrosis factor α-mediated apoptosis requires Ras and the activation of mitogen-activated protein kinase. J Biol Chem 1996, 271:14560–14566
11. Moscatelli D, Joseph-Silverstein J, Presta M, Rifkin DB: Multiple forms of an angiogenesis factor: basic fibroblast growth factor. Biochimie 1988, 70:83–87
12. Florkiewicz RZ, Sommer A: Human basic fibroblast growth factor gene encodes four polypeptides: three initiate translation from non-AUG codons. Proc Natl Acad Sci USA 1989, 86:3978–3981
13. Piotrowicz RS, Martin JL, Dillmann WH, Levin EG: The 27-kDa heat shock protein facilitates basic fibroblast growth factor release from endothelial cells. J Biol Chem 1997, 272:7042–7047
14. Ding L, Donate F, Parry GC, Guan X, Maher P, Levin EG: Inhibition of cell migration and angiogenesis by the amino-terminal fragment of 24kDa basic fibroblast growth factor. J Biol Chem 2002, 277:31056–31061
15. Traver D, Zon LI: Walking the walk: migration and other common themes in blood and vascular development. Cell 2002, 108:731–734
16. Moore MA: The role of chemoattraction in cancer metastases. Bioessays 2001, 23:674–676
17. Mollabashy A, Scarborough M: The mechanism of metastasis. Orthop Clin North Am 2000, 31:529–535
18. Montell DJ: Developmental regulation of cell migration: insight from a genetic approach in Drosophila. Cell Biochem Biophys 1999, 31: 219–229
19. Westermann J, Ehlers EM, Exton MS, Kaiser M, Bode U: Migration of naive, effector, and memory T cells: implications for the regulation of immune responses. Immunol Rev 2001, 184:20–37
20. Kunkel EJ, Butcher EC: Chemokines and the tissue-specific migration of lymphocytes. Immunity 2002, 16:1–4
21. Lev S: Molecular aspects of retinal degenerative diseases. Cell Mol Neurobiol 2001, 21:575–589
22. Cai J, Boulton M: The pathogenesis of diabetic retinopathy: old concepts and new questions. Eye 2002, 16:242–260
23. Lehr HA, Leunig M, Menger MD, Nolte D, Messmer K: Dorsal skinfold chamber technique for intravital microscopy in nude mice. Am J Pathol 1993, 143:1055–1062
24. Borgström P, Hughes G, Hansell P, Wolitzky B, Sriramarao P: Leukocyte adhesion in angiogenic blood vessels: role of E-selectin P-selectin and b2 integrin in lymphotoxin-mediated leukocyte recruitment in tumor microvessels. J Clin Invest 1997, 99:2246–2253
25. Borgström P, Hillan KJ, Sriramarao P, Ferrara N: Complete inhibition of angiogenesis and growth of microtumors by anti-VEGF neutralizing antibody: novel concepts of angiostatic therapy from intravital videomicroscopy. Cancer Res 1996, 56:4032–4039
26. Sriramarao P, DiScipio RG: Deposition of complement C3 and Factor H in tissue traumatized by burn injury. Immunopharmacology 1999, 142:195–202
27. DiScipio RG, Daffern PJ, Jagels MA, Broide DH, Sriramarao P: A comparison of C3a and C5a mediated stable adhesion of rolling eosinophil in postcapillary venules and transendothelial migration in vitro and in vivo. J Immunol 1999, 162:1127–1136
28. Kerbel R, Folkman J: Clinical translation of angiogenesis inhibitors. Nat Rev Cancer 2002, 2:727–739
29. Hood JD, Bednarski M, Frausto R, Guccione S, Reisfeld RA, Xiang R, Cheresh DA: Tumor regression by targeted gene delivery to the neovasculature. Science 2002, 296:2404–2407
30. Mitchison TJ, Cramer LP: Actin-based cell motility and cell locomotion. Cell 1996, 84:371–379
31. Lauffenburger DA, Horwitz AF: Cell migration: a physically integrated molecular process. Cell 1996, 84:359–369